



1-1-2021

Multimessenger gamma-ray and neutrino coincidence alerts using hawc and icecube subthreshold data

H. A. Ayala Solares

Pennsylvania State University

S. Coutu

Pennsylvania State University

J. J. DeLaunay

Pennsylvania State University

D. B. Fox

Pennsylvania State University

T. Grégoire

Pennsylvania State University

See next page for additional authors

Follow this and additional works at: https://ecommons.luc.edu/physics_facpubs

Recommended Citation

Solares, H. A. Ayala; Coutu, S.; DeLaunay, J. J.; Fox, D. B.; Grégoire, T.; Keivani, A.; Krauß, F.; Mostafá, M.; Murase, K.; Turley, C. F.; Albert, A.; Alfaro, R.; Alvarez, C.; Angeles Camacho, J. R.; Arteaga-Velázquez, J. C.; Arunbabu, K. P.; Rojas, D. Avila; Belmont-Moreno, E.; Brisbois, C.; Caballero-Mora, K. S.; Carramiñana, A.; Casanova, S.; Cotti, U.; De la Fuente, E.; and Hernandez, R. Diaz, "Multimessenger gamma-ray and neutrino coincidence alerts using hawc and icecube subthreshold data" (2021). *Physics: Faculty Publications and Other Works*. 99.

https://ecommons.luc.edu/physics_facpubs/99

Authors

H. A. Ayala Solares, S. Coutu, J. J. DeLaunay, D. B. Fox, T. Grégoire, A. Keivani, F. Krauß, M. Mostafá, K. Murase, C. F. Turley, A. Albert, R. Alfaro, C. Alvarez, J. R. Angeles Camacho, J. C. Arteaga-Velázquez, K. P. Arunbabu, D. Avila Rojas, E. Belmont-Moreno, C. Brisbois, K. S. Caballero-Mora, A. Carramiñana, S. Casanova, U. Cotti, E. De la Fuente, and R. Diaz Hernandez



Multimessenger Gamma-Ray and Neutrino Coincidence Alerts Using HAWC and IceCube Subthreshold Data

H. A. Ayala Solares¹, S. Couto¹, J. J. DeLaunay¹, D. B. Fox¹, T. Grégoire¹, A. Keivani^{2,3}, F. Krauß¹, M. Mostafá¹, K. Murase¹, C. F. Turley¹

AMON Team,

A. Albert⁴, R. Alfaro⁵, C. Alvarez⁶, J. R. Angeles Camacho⁵, J. C. Arteaga-Velázquez⁷, K. P. Arunbabu⁸, D. Avila Rojas⁵, E. Belmont-Moreno⁵, C. Brisbois⁹, K. S. Caballero-Mora⁶, A. Carramíñana¹⁰, S. Casanova¹¹, U. Cotti⁷, E. De la Fuente¹², R. Diaz Hernandez¹⁰, B. L. Dingus⁴, M. A. DuVernois¹³, M. Durocher⁴, J. C. Díaz-Vélez¹², C. Espinoza⁵, K. L. Fan⁹, H. Fleischhack¹⁴, N. Fraija¹⁵, A. Galván-Gámez¹⁵, D. Garcia⁵, J. A. García-González¹⁵, F. Garfias¹⁵, M. M. González¹⁵, J. A. Goodman⁹, J. P. Harding⁴, B. Hona¹⁶, D. Huang¹⁴, F. Hueyotl-Zahuantitla⁶, P. Hüntemeyer¹⁴, A. Iriarte¹⁵, A. Jardin-Blicq^{17,18,19}, V. Joshi²⁰, H. León Vargas⁵, J. T. Linnemann²¹, A. L. Longinotti¹⁰, G. Luis-Raya²², J. Lundeen²¹, K. Malone⁴, O. Martinez²³, I. Martinez-Castellanos⁹, J. Martínez-Castro²⁴, J. A. Matthews²⁵, P. Miranda-Romagnoli²⁶, E. Moreno²³, L. Nellen²⁷, M. Newbold¹⁶, M. U. Nisa²¹, R. Noriega-Papaqui²⁶, A. Peisker²¹, E. G. Pérez-Pérez²², C. D. Rho²⁸, D. Rosa-González¹⁰, H. Salazar²³, F. Salesa Greus^{11,29}, A. Sandoval⁵, A. J. Smith⁹, R. W. Springer¹⁶, K. Tollefson²¹, I. Torres¹⁰, R. Torres-Escobedo¹², F. Ureña-Mena¹⁰, L. Villaseñor²³, T. Weisgarber³⁰, E. Willox⁹, A. Zepeda³¹, H. Zhou³², C. de León⁷

HAWC Collaboration,

and

M. G. Aartsen³³, R. Abbasi³⁴, M. Ackermann³⁵, J. Adams³³, J. A. Aguilar³⁶, M. Ahlers³⁷, M. Ahrens³⁸, C. Alispach³⁹, N. M. Amin⁴⁰, K. Andeen⁴¹, T. Anderson¹, I. Ansseau³⁶, G. Anton²⁰, C. Argüelles⁴², J. Auffenberg⁴³, S. Axani⁴², H. Bagherpour³³, X. Bai⁴⁴, A. Balagopal V.⁴⁵, A. Barbano³⁹, S. W. Barwick⁴⁶, B. Bastian³⁵, V. Basu⁴⁷, V. Baum⁴⁸, S. Baur³⁶, R. Bay⁴⁹, J. J. Beatty^{50,51}, K.-H. Becker⁵², J. Becker Tjus⁵³, S. BenZvi⁵⁴, D. Berley⁹, E. Bernardini^{35,85}, D. Z. Besson^{55,86}, G. Binder^{49,56}, D. Bindig⁵², E. Blaufuss⁹, S. Blot³⁵, C. Bohm³⁸, S. Böser⁴⁸, O. Botner⁵⁷, J. Böttcher⁴³, E. Bourbeau³⁷, J. Bourbeau⁴⁷, F. Bradascio³⁵, J. Braun⁴⁷, S. Bron³⁹, J. Brostean-Kaiser³⁵, A. Burgman⁵⁷, J. Buscher⁴³, R. S. Busse⁵⁸, T. Carver³⁹, C. Chen⁵⁹, E. Cheung⁹, D. Chirkin⁴⁷, S. Choi⁶⁰, B. A. Clark²¹, K. Clark⁶¹, L. Classen⁵⁸, A. Coleman⁴⁰, G. H. Collin⁴², J. M. Conrad⁴², P. Coppin⁶², P. Correa⁶², D. F. Cowen^{1,63}, R. Cross⁵⁴, P. Dave⁵⁹, C. De Clercq⁶², H. Dembinski⁴⁰, K. Deoskar³⁸, S. De Ridder⁶⁴, A. Desai⁴⁷, P. Desiati⁴⁷, K. D. de Vries⁶², G. de Wasseige⁶², M. de With⁶⁵, T. DeYoung²¹, S. Dharani⁴³, A. Diaz⁴², H. Djurmovic⁴⁵, M. Dunkman¹, E. Dvorak⁴⁴, T. Ehrhardt⁴⁸, P. Eller¹, R. Engel⁴⁵, P. A. Evenson⁴⁰, S. Fahey⁴⁷, A. R. Fazely⁶⁶, J. Felde⁹, A. Fienberg¹, K. Filimonov⁴⁹, C. Finley³⁸, A. Franckowiak³⁵, E. Friedman⁹, A. Fritz⁴⁸, T. K. Gaisser⁴⁰, J. Gallagher⁶⁷, E. Ganster⁴³, S. Garrappa³⁵, L. Gerhardt⁵⁶, T. Glauch⁶⁸, T. Glüsenkamp²⁰, A. Goldschmidt⁵⁶, J. G. Gonzalez⁴⁰, D. Grant²¹, Z. Griffith⁴⁷, S. Griswold⁵⁴, M. Günder⁴³, M. Gündüz⁵³, C. Haack⁴³, A. Hallgren⁵⁷, R. Halliday²¹, L. Halve⁴³, F. Halzen⁴⁷, K. Hanson⁴⁷, J. Hardin⁴⁷, A. Haungs⁴⁵, S. Hauser⁴³, D. Hebecker⁶⁵, D. Heereman³⁶, P. Heix⁴³, K. Helbing⁵², R. Hellauer⁹, F. Henningsen⁶⁸, S. Hickford⁵², J. Hignight⁶⁹, C. Hill⁷⁰, G. C. Hill⁷¹, K. D. Hoffman⁹, R. Hoffmann⁵², T. Hoinka⁷², B. Hokanson-Fasig⁴⁷, K. Hoshina^{47,87}, F. Huang¹, M. Huber⁶⁸, T. Huber^{45,35}, K. Hultqvist³⁸, M. Hünnefeld⁷², R. Hussain⁴⁷, S. In⁶⁰, N. Iovine³⁶, A. Ishihara⁷⁰, M. Jansson³⁸, G. S. Japaridze⁷³, M. Jeong⁶⁰, B. J. P. Jones⁷⁴, F. Jonske⁴³, R. Joppe⁴³, D. Kang⁴⁵, W. Kang⁶⁰, A. Kappes⁵⁸, D. Kappesser⁴⁸, T. Karg³⁵, M. Karl⁶⁸, A. Karle⁴⁷, U. Katz²⁰, M. Kauer⁴⁷, M. Kellermann[,], J. L. Kelley⁴⁷, A. Kheirandish¹, J. Kim⁶⁰, K. Kin⁷⁰, T. Kintscher³⁵, J. Kiryluk⁷⁵, T. Kittler²⁰, S. R. Klein^{49,56}, R. Koirlala⁴⁰, H. Kolanoski⁶⁵, L. Köpke⁴⁸, C. Kopper²¹, S. Kopper⁷⁶, D. J. Koskinen³⁷, P. Koundal⁴⁵, M. Kowalski^{65,35}, K. Krings⁶⁸, G. Krückl⁴⁸, N. Kulacz⁶⁹, N. Kurahashi⁷⁷, A. Kyriacou⁷¹, J. L. Lanfranchi¹, M. J. Larson⁹, F. Lauber⁵², J. P. Lazar⁴⁷, K. Leonard⁴⁷, A. Leszczyńska⁴⁵, Y. Li¹, Q. R. Liu⁴⁷, E. Lohfink⁴⁸, C. J. Lozano Mariscal⁵⁸, L. Lu⁷⁰, F. Lucarelli³⁹, A. Ludwig⁷⁸, J. Lünemann⁶², W. Luszczak⁴⁷, Y. Lyu^{49,56}, W. Y. Ma³⁵, J. Madsen⁷⁹, G. Maggi⁶², K. B. M. Mahn²¹, Y. Makino⁴⁷, P. Mallik⁴³, S. Mancina⁴⁷, I. C. Mariş³⁶, R. Maruyama⁸⁰, K. Mase⁷⁰, R. Maunu⁹, F. McNally⁸¹, K. Meagher⁴⁷, M. Medici³⁷, A. Medina⁵¹, M. Meier⁷⁰, S. Meighen-Berger⁶⁸, J. Merz⁴³, T. Meures³⁶, J. Micallef²¹, D. Mockler³⁶, G. Momenté⁴⁸, T. Montaruli³⁹, R. W. Moore⁶⁹, R. Morse⁴⁷, M. Moulai⁴², P. Muth⁴³, R. Nagai⁷⁰, U. Naumann⁵², G. Neer²¹, L. V. Nguyen²¹, H. Niederhausen⁶⁸, S. C. Nowicki²¹, D. R. Nygren⁵⁶, A. Obertacke Pollmann⁵², M. Oehler⁴⁵, A. Olivas⁹, A. O'Murchadha³⁶, E. O'Sullivan³⁸, H. Pandya⁴⁰, D. V. Pankova¹, N. Park⁴⁷, G. K. Parker⁷⁴, E. N. Paudel⁴⁰, P. Peiffer⁴⁸, C. Pérez de los Heros⁵⁷, S. Philippe⁴³, D. Pieloth⁷², S. Pieper⁵², E. Pinat³⁶, A. Pizzuto⁴⁷, M. Plum⁴¹, Y. Popovych⁴³, A. Porcelli⁶⁴, M. Prado Rodriguez⁴⁷, P. B. Price⁴⁹, G. T. Przybylski⁵⁶, C. Raab³⁶, A. Raissi³³, M. Rameez³⁷, L. Rauch³⁵, K. Rawlins⁸², I. C. Rea⁶⁸, A. Rehman⁴⁰, R. Reimann⁴³, B. Relethford⁷⁷, M. Renschler⁴⁵, G. Renzi³⁶, E. Resconi⁶⁸, W. Rhode⁷², M. Richman⁷⁷, B. Riedel⁴⁷, S. Robertson^{49,56}, G. Roellinghoff⁶⁰, M. Rongen⁴³, C. Rott⁶⁰, T. Ruhe⁷², D. Ryckbosch⁶⁴, D. Rysewyk Cantu²¹, I. Safa⁴⁷, S. E. Sanchez Herrera²¹, A. Sandrock⁷², J. Sandroos⁴⁸, M. Santander⁷⁶, S. Sarkar⁸³, S. Sarkar⁶⁹, K. Satalecka³⁵, M. Scharf⁴³, M. Schaufel⁴³, H. Schieler⁴⁵, P. Schlunder⁷², T. Schmidt⁹, A. Schneider⁴⁷, J. Schneider²⁰, F. G. Schröder^{45,40}, L. Schumacher⁴³, S. Sclafani⁷⁷, D. Seckel⁴⁰, S. Seunarine⁷⁹, S. Shefali⁴³, M. Silva⁴⁷, B. Smithers⁷⁴, R. Snihur⁴⁷, J. Soedingrekso⁷², D. Soldin⁴⁰, M. Song⁹, G. M. Spiczak⁷⁹, C. Spiering³⁵, J. Stachurska³⁵, M. Stamatikos⁵¹, T. Staney³⁵, R. Stein³⁵, J. Stettner⁴³, A. Steuer⁴⁸, T. Stezelberger⁵⁶,

R. G. Stokstad⁵⁶, N. L. Strotjohann³⁵^{ID}, T. Stürwald⁴³, T. Stuttard³⁷, G. W. Sullivan⁹, I. Taboada⁵⁹, F. Tenholt⁵³, S. Ter-Antonyan⁶⁶, A. Terliuk³⁵, S. Tilav⁴⁰, L. Tomankova⁵³, C. Tönnis⁸⁴, S. Toscano³⁶, D. Tosi⁴⁷, A. Trettin³⁵, M. Tselengidou²⁰, C. F. Tung⁵⁹, A. Turcati⁶⁸, R. Turcotte⁴⁵, B. Ty⁴⁷, E. Unger⁵⁷, M. A. Unland Elorrieta⁵⁸, M. Usner³⁵, J. Vandenbroucke⁴⁷^{ID}, W. Van Driessche⁶⁴, D. van Eijk⁴⁷, N. van Eijndhoven⁶², D. Vannerom⁴², J. van Santen³⁵, S. Verpoest⁶⁴, M. Vraeghe⁶⁴, C. Walck³⁸, A. Wallace⁷¹, M. Wallraff⁴³, T. B. Watson⁷⁴, C. Weaver⁶⁹, A. Weindl⁴⁵, M. J. Weiss¹, J. Weldert⁴⁸, C. Wendt⁴⁷, J. Werthebach⁷², B. J. Whelan⁷¹, N. Whitehorn⁷⁸^{ID}, K. Wiebe⁴⁸, C. H. Wiebusch⁴³, D. R. Williams⁷⁶, L. Wills⁷⁷, M. Wolf⁶⁸, T. R. Wood⁶⁹, K. Woschnagg⁴⁹, G. Wrede²⁰, J. Wulff⁵³, X. W. Xu⁶⁶, Y. Xu⁷⁵, J. P. Yanez⁶⁹, S. Yoshida⁷⁰, T. Yuan⁴⁷, Z. Zhang⁷⁵, and M. Zöcklein⁴³

IceCube Collaboration

¹ Department of Physics, Pennsylvania State University, University Park, PA 16802, USA; hgayala@psu.edu² Department of Physics, Columbia University, New York, NY 10027, USA³ Columbia Astrophysics Laboratory, Columbia University, New York, NY 10027, USA⁴ Physics Division, Los Alamos National Laboratory, Los Alamos, NM, USA⁵ Instituto de Física, Universidad Nacional Autónoma de México, Ciudad de México, México⁶ Universidad Autónoma de Chiapas, Tuxtla Gutiérrez, Chiapas, México⁷ Universidad Michoacana de San Nicolás de Hidalgo, Morelia, México⁸ Instituto de Geofísica, Universidad Nacional Autónoma de México, Ciudad de México, México⁹ Department of Physics, University of Maryland, College Park, MD 20742, USA¹⁰ Instituto Nacional de Astrofísica, Óptica y Electrónica, Puebla, México¹¹ Institute of Nuclear Physics, Polish Academy of Sciences, PL-31342 IFJ-PAN, Krakow, Poland¹² Departamento de Física, Centro Universitario de Ciencias Exactas e Ingenierías, Universidad de Guadalajara, Guadalajara, México¹³ Department of Physics, University of Wisconsin–Madison, Madison, WI 53706, USA¹⁴ Department of Physics, Michigan Technological University, Houghton, MI, USA¹⁵ Instituto de Astronomía, Universidad Nacional Autónoma de México, Ciudad de México, México¹⁶ Department of Physics and Astronomy, University of Utah, Salt Lake City, UT, USA¹⁷ Max-Planck Institute for Nuclear Physics, D-69117 Heidelberg, Germany¹⁸ Department of Physics, Faculty of Science, Chulalongkorn University, Bangkok 10330, Thailand¹⁹ National Astronomical Research Institute of Thailand (Public Organization), Chiang Mai 50180, Thailand²⁰ Erlangen Centre for Astroparticle Physics, Friedrich-Alexander-Universität Erlangen-Nürnberg, D-91058 Erlangen, Germany²¹ Department of Physics and Astronomy, Michigan State University, East Lansing, MI 48824, USA²² Universidad Politécnica de Pachuca, Pachuca, Hgo, México²³ Facultad de Ciencias Físico Matemáticas, Benemérita Universidad Autónoma de Puebla, Puebla, México²⁴ Centro de Investigación en Computación, Instituto Politécnico Nacional, Mexico City, Mexico²⁵ Department of Physics and Astronomy, University of New Mexico, Albuquerque, NM, USA²⁶ Universidad Autónoma del Estado de Hidalgo, Pachuca, México²⁷ Instituto de Ciencias Nucleares, Universidad Nacional Autónoma de México, Ciudad de México, México²⁸ Natural Science Research Institute, University of Seoul, Seoul, Republic of Korea²⁹ Instituto de Física Corpuscular, CSIC, Universitat de València, E-46980, Paterna, Valencia, Spain³⁰ Department of Chemistry and Physics, California University of Pennsylvania, California, PA, USA³¹ Physics Department, Centro de Investigación y de Estudios Avanzados del IPN, Mexico City, DF, Mexico³² Tsung-Dao Lee Institute & School of Physics and Astronomy, Shanghai Jiao Tong University, Shanghai, People's Republic of China³³ Department of Physics and Astronomy, University of Canterbury, Private Bag 4800, Christchurch, New Zealand³⁴ Department of Physics, Loyola University Chicago, Chicago, IL 60660, USA³⁵ DESY, D-15738 Zeuthen, Germany³⁶ Université Libre de Bruxelles, Science Faculty CP230, B-1050 Brussels, Belgium³⁷ Niels Bohr Institute, University of Copenhagen, DK-2100 Copenhagen, Denmark³⁸ Oskar Klein Centre and Department of Physics, Stockholm University, SE-10691 Stockholm, Sweden³⁹ Département de physique nucléaire et corpusculaire, Université de Genève, CH-1211 Genève, Switzerland⁴⁰ Bartol Research Institute and Department of Physics and Astronomy, University of Delaware, Newark, DE 19716, USA⁴¹ Department of Physics, Marquette University, Milwaukee, WI 53201, USA⁴² Department of Physics, Massachusetts Institute of Technology, Cambridge, MA 02139, USA⁴³ III. Physikalisch Institut, RWTH Aachen University, D-52056 Aachen, Germany⁴⁴ Physics Department, South Dakota School of Mines and Technology, Rapid City, SD 57701, USA⁴⁵ Karlsruhe Institute of Technology, Institut für Kernphysik, D-76021 Karlsruhe, Germany⁴⁶ Department of Physics and Astronomy, University of California, Irvine, CA 92697, USA⁴⁷ Department of Physics and Wisconsin IceCube Particle Astrophysics Center, University of Wisconsin, Madison, WI 53706, USA⁴⁸ Institute of Physics, University of Mainz, Staudinger Weg 7, D-55099 Mainz, Germany⁴⁹ Department of Physics, University of California, Berkeley, CA 94720, USA⁵⁰ Department of Astronomy, Ohio State University, Columbus, OH 43210, USA⁵¹ Department of Physics and Center for Cosmology and Astro-Particle Physics, Ohio State University, Columbus, OH 43210, USA⁵² Department of Physics, University of Wuppertal, D-42119 Wuppertal, Germany⁵³ Fakultät für Physik & Astronomie, Ruhr-Universität Bochum, D-44780 Bochum, Germany⁵⁴ Department of Physics and Astronomy, University of Rochester, Rochester, NY 14627, USA⁵⁵ Department of Physics and Astronomy, University of Kansas, Lawrence, KS 66045, USA⁵⁶ Lawrence Berkeley National Laboratory, Berkeley, CA 94720, USA⁵⁷ Department of Physics and Astronomy, Uppsala University, Box 516, SE-75120 Uppsala, Sweden⁵⁸ Institut für Kernphysik, Westfälische Wilhelms-Universität Münster, D-48149 Münster, Germany⁵⁹ School of Physics and Center for Relativistic Astrophysics, Georgia Institute of Technology, Atlanta, GA 30332, USA⁶⁰ Department of Physics, Sungkyunkwan University, Suwon 16419, Republic of Korea⁶¹ SNOLAB, 1039 Regional Road 24, Creighton Mine 9, Lively, ON, P3Y 1N2, Canada⁶² Vrije Universiteit Brussel (VUB), Dienst ELEM, B-1050 Brussels, Belgium⁶³ Department of Astronomy and Astrophysics, Pennsylvania State University, University Park, PA 16802, USA⁶⁴ Department of Physics and Astronomy, University of Gent, B-9000 Gent, Belgium

- ⁶⁵ Institut für Physik, Humboldt-Universität zu Berlin, D-12489 Berlin, Germany
⁶⁶ Department of Physics, Southern University, Baton Rouge, LA 70813, USA
⁶⁷ Department of Astronomy, University of Wisconsin, Madison, WI 53706, USA
⁶⁸ Physik-department, Technische Universität München, D-85748 Garching, Germany
⁶⁹ Department of Physics, University of Alberta, Edmonton, AB, T6G 2E1, Canada
⁷⁰ Department of Physics and Institute for Global Prominent Research, Chiba University, Chiba 263-8522, Japan
⁷¹ Department of Physics, University of Adelaide, Adelaide, 5005, Australia
⁷² Department of Physics, TU Dortmund University, D-44221 Dortmund, Germany
⁷³ CTSPS, Clark-Atlanta University, Atlanta, GA 30314, USA
⁷⁴ Department of Physics, University of Texas at Arlington, 502 Yates Street, Science Hall Room 108, Box 19059, Arlington, TX 76019, USA
⁷⁵ Department of Physics and Astronomy, Stony Brook University, Stony Brook, NY 11794-3800, USA
⁷⁶ Department of Physics and Astronomy, University of Alabama, Tuscaloosa, AL 35487, USA
⁷⁷ Department of Physics, Drexel University, 3141 Chestnut Street, Philadelphia, PA 19104, USA
⁷⁸ Department of Physics and Astronomy, UCLA, Los Angeles, CA 90095, USA
⁷⁹ Department of Physics, University of Wisconsin, River Falls, WI 54022, USA
⁸⁰ Department of Physics, Yale University, New Haven, CT 06520, USA
⁸¹ Department of Physics, Mercer University, Macon, GA 31207-0001, USA
⁸² Department of Physics and Astronomy, University of Alaska Anchorage, 3211 Providence Drive, Anchorage, AK 99508, USA
⁸³ Department of Physics, University of Oxford, Parks Road, Oxford OX1 3PU, UK
⁸⁴ Institute of Basic Science, Sungkyunkwan University, Suwon 16419, Republic of Korea

Received 2020 August 24; revised 2020 November 9; accepted 2020 November 13; published 2021 January 7

Abstract

The High Altitude Water Cerenkov (HAWC) and IceCube observatories, through the Astrophysical Multimessenger Observatory Network (AMON) framework, have developed a multimessenger joint search for extragalactic astrophysical sources. This analysis looks for sources that emit both cosmic neutrinos and gamma rays that are produced in photohadronic or hadronic interactions. The AMON system is running continuously, receiving subthreshold data (i.e., data that are not suited on their own to do astrophysical searches) from HAWC and IceCube, and combining them in real time. Here we present the analysis algorithm, as well as results from archival data collected between 2015 June and 2018 August, with a total live time of 3.0 yr. During this period we found two coincident events that have a false-alarm rate (FAR) of <1 coincidence yr^{-1} , consistent with the background expectations. The real-time implementation of the analysis in the AMON system began on 2019 November 20 and issues alerts to the community through the Gamma-ray Coordinates Network with an FAR threshold of <4 coincidences yr^{-1} .

Unified Astronomy Thesaurus concepts: Cosmological neutrinos (338); Gamma-rays (637); High energy astrophysics (739)

1. Introduction

The coincident detection of gravitational waves and electromagnetic radiation (Abbott et al. 2017), as well as the evidence found for a neutrino coincident with a gamma-ray flare from the blazar TXS 0506+056 (Aartsen et al. 2018), have shown the potential of multimessenger astrophysics. The ability to combine data from different observatories in real time or near-real time is driving this new era in astrophysics. The Astrophysical Multimessenger Observatory Network (AMON) has been created to facilitate the interaction of different observatories, create a framework for analyses with distinct data sets across multiple experiments, and notify the astrophysical community of any interesting events worthy of follow-up (Smith et al. 2013; Ayala Solares et al. 2020).⁸⁸

AMON focuses on using data that are below the discovery threshold of individual observatories. These events by themselves are heavily background-dominated, which complicates a search for astrophysical sources. By statistically combining the temporal and/or spatial information of these subthreshold events provided by different detectors, AMON aims to recover the signal events that are hidden among the

background of each single observatory. Two multimessenger analyses were previously developed combining gamma-ray data from Fermi-LAT with neutrino data: one using IceCube data (Turley et al. 2018) and the other using ANTARES data (Ayala Solares et al. 2019).⁸⁹ The Fermi-LAT and ANTARES coincidence search started running in real time in 2019 April and has issued two alerts to date (see GCN circulars Turley 2020a, 2020b).

In this work, we focus on a new coincidence analysis combining information from the High Altitude Water Cerenkov (HAWC) Gamma-Ray Observatory (Abeysekara et al. 2017) and the IceCube Neutrino Observatory (Aartsen et al. 2017a) using the AMON infrastructure. This new multimessenger channel has been operational as a real-time coincidence search since 2019 December.

The purpose of this analysis is to search for hadronic accelerators that produce both gamma rays and neutrinos as secondary particles, with an emphasis on transient events. The accelerated cosmic rays can interact with target material surrounding the environment of the sources or with radiation fields. These interactions produce charged and neutral pions. Charged pions predominantly decay via $\pi^+ \rightarrow \mu^+ + \nu_\mu$, followed by the decay of the muon as $\mu^+ \rightarrow e^+ + \nu_e + \bar{\nu}_\mu$ (and charge conjugate). Neutral pions decay into two gamma-

⁸⁵ Also at Università di Padova, I-35131 Padova, Italy.

⁸⁶ Also at National Research Nuclear University, Moscow Engineering Physics Institute (MEPhI), Moscow 115409, Russia.

⁸⁷ Earthquake Research Institute, University of Tokyo, Bunkyo, Tokyo 113-0032, Japan.

⁸⁸ AMON website: <https://www.amon.psu.edu/>.

⁸⁹ Although what constitutes the data depends on the groups or collaborations, in general, the position and time of the events are always used. Other information is added if available.

ray photons, $\pi^0 \rightarrow \gamma + \gamma$. The ratio between charged and neutral pions depends on the type of interaction of the cosmic rays with the targets. If the interaction occurs with electromagnetic radiation, the interaction will be photohadronic, which produces charged and neutral pions with probabilities of one-third and two-thirds, after considering both resonant and nonresonant pion productions. If the pions originate from interactions of cosmic rays with matter, the probability of producing charged and neutral pions is one-third for each type of pion (Biehl et al. 2019). A useful relation between the fluxes of gamma rays (F_γ) and neutrinos (F_{ν_α}) is expressed as

$$E_\gamma F_\gamma(E_\gamma) \approx e^{-\frac{d}{\lambda_{\gamma\gamma}}} \frac{2}{3K} \sum_{\nu_\alpha} E_\nu F_{\nu_\alpha}(E_\nu), \quad (1)$$

where $E_\gamma \approx 2E_\nu$ are the gamma-ray and neutrino energies; α corresponds to the neutrino flavor; K is the ratio of charged to neutral pions, with $K = 1$ for photohadronic interactions and $K = 2$ for hadronuclear interactions; d is the distance to the source; and $\lambda_{\gamma\gamma}$ accounts for the attenuation of gamma rays due to their interaction with the extragalactic background light (EBL; see Murase et al. 2013 and Ahlers & Murase 2014).

In this paper, we present the algorithm and analysis to search for possible sources of gamma rays and neutrinos by looking at HAWC's and IceCube's subthreshold data. In Section 2, we briefly describe the detectors and their data. In Section 3, we present the statistical method and provide the false-alarm rate (FAR), sensitivities, and discovery potentials.

In Section 4, we present the results obtained using 3 yr of archival data, including upper limits for the same period of time for the total isotropic equivalent energy and source rate density parameter space. Finally, we conclude and discuss the implementation of the analysis in real time using the AMON framework.

2. HAWC and IceCube Detectors and Data Sets

The HAWC and IceCube are two detectors that focus on high-energy astrophysics, searching for sources that accelerate cosmic rays. Both detectors use the Cerenkov technique, where photomultipliers are used to detect the Cerenkov light produced by the passage of secondary charged relativistic particles—from gamma-ray, neutrino, and cosmic-ray showers—through a medium. The HAWC uses water as the medium, while IceCube uses the Antarctic ice.

Due to the attenuation of gamma rays on the extragalactic background photons, the signal from a source might not be significantly detected above background in the HAWC data. However, if IceCube neutrino events are found in spatiotemporal coincidence with a subthreshold HAWC hot spot, this might become an interesting coincidence that could be followed up by other observatories. In addition, the uncertainty region of HAWC events is generally smaller compared to IceCube events, which can give a better localization of a potential joint source.

2.1. High-energy Gamma Rays from HAWC

The HAWC observatory is a high-energy gamma-ray detector located in central Mexico. The complete detector has been in operation since 2015 March. The HAWC has a large field of view, covering two-thirds of the sky every day with a high-duty cycle in the decl. range from -26° to 64° . It is mainly sensitive to gamma rays in the energy range between 300 GeV and 100 TeV. It has an angular resolution of 0.2° – 1°

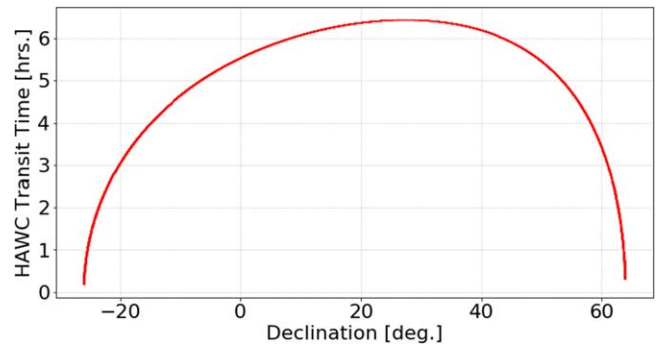


Figure 1. Duration of a transit of a point in the sky as a function of decl. above the HAWC detector, applying a zenith angle cut of $<45^\circ$.

(68% containment) that depends on the energy of the event, its zenith angle, and the size of the shower footprint measured by HAWC (Abeysekara et al. 2017).

We select locations of excess exceeding a given significance threshold—called “hot spots”—from the HAWC data to be used as inputs to the combined search. Hot spots are defined as locations in the sky with a cluster of events above the estimated cosmic-ray background level and measured by the significance (excess above the background). They are identified during one full transit of that sky location above the detector. The main hot-spot parameters AMON receives are the position coordinates and their uncertainty; the significance value, with a minimum of 2.75σ (threshold defined by HAWC); and the start and stop times of the transit. The duration of the transits are decl.-dependent, as shown in Figure 1. Since we are searching for unknown sources or sources that cannot be significantly detected above the background, we mask the data from the following parts of the sky above HAWC: the Galactic plane ($b < |3^\circ|$), the Crab Nebula, Geminga, Monogem, Mkr 421, and Mkr 501. The current rate of these hot spots received by AMON is ~ 800 day $^{-1}$.

2.2. High-energy Neutrinos from IceCube

The IceCube observatory is a detector of high-energy neutrinos located at the South Pole (Aartsen et al. 2017a). It became fully operational in 2011 after 7 yr of construction. IceCube first observed the high-energy astrophysical neutrino flux in 2013 (Aartsen et al. 2013).

IceCube can search for neutrinos from the whole sky, though it is more sensitive to sources from the northern celestial hemisphere, since the Earth helps reduce the atmospheric background in IceCube. This is an advantage in this analysis, since HAWC is primarily sensitive in the northern sky. IceCube is sensitive to energies that can reach up to 1 EeV near the horizon (decl. of 0°). The angular resolution depends on the topology of the events inside the detector. Two main topologies are observed: track events and cascade events. Track events are mostly induced by charged-current muon–neutrino interactions. These tracks can have a length of several kilometers and most of the time extend beyond the detector volume. The track events have a median angular resolution of $\sim 0.4^\circ$ above 100 TeV. Cascade events are produced by the other types of neutrinos or neutral-current interactions of any neutrino type. They have better energy resolution compared to tracks, since the energy deposited by the events is completely contained inside the detector. Their angular resolution,

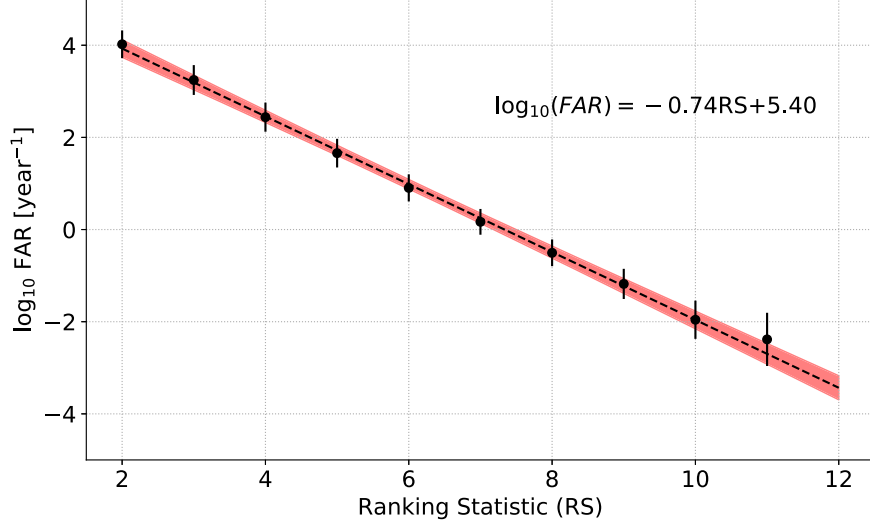


Figure 2. The FAR as a function of the ranking statistic obtained from the scrambled data sets. The width of the band (in red) is the 1σ statistical uncertainty. The function in the graph will be used to select alerts that will be sent to the Galactic Coordinates Network (<https://gcn.gsfc.nasa.gov/>). An FAR of 1 yr^{-1} is obtained with a ranking statistic value of 7.3.

however, is $>10^\circ$ with current reconstruction methods (Aartsen et al. 2017b).

The IceCube candidate events sent to AMON consist of single throughgoing tracks. These events can have energies above 0.1 TeV for upgoing events, while downgoing events can have energies above 100 TeV. Lower-energy events are more likely to be background events. The parameters consist of the sky position and its uncertainty, the time of the event, and the reconstructed energy or boosted decision tree (BDT)⁹⁰ score (see Section 3 of Aartsen et al. 2017b), depending on whether the event is in the northern or southern hemisphere, respectively, and can be used to calculate the background p -value of the event. The current rate of events received by AMON is $\sim 650 \text{ day}^{-1}$.

3. Method

The coincidence analysis is applied to events satisfying two criteria. The first is a temporal selection requiring the neutrino events to arrive within the transit time of the HAWC hot spot. Second, we select neutrinos that are within a radius of 3.5° from the HAWC hot-spot localization.⁹¹ After the neutrino events have passed the selection criteria, we calculate a statistic to rank the coincident events. The rate of coincidences after passing the criteria is $\sim 100 \text{ day}^{-1}$. This ranking statistic is based on Fisher’s method (Fisher 1938), where we combine all the information that we have from the events. It is defined as

$$\chi^2_{6+2n_\nu} = -2 \ln[p_\lambda p_{\text{HAWC}} p_{\text{cluster}} \prod_i^{n_\nu} p_{\text{IC},i}], \quad (2)$$

where the number of degrees of freedom is $6 + 2n_\nu$ (as described below). The quantity p_λ quantifies the overlap of the spatial uncertainties of the events. The value p_{HAWC} is the probability of the HAWC event being compatible with a background fluctuation. Since we can expect more than one IceCube candidate event in the time window (i.e., the HAWC transit period), we can calculate the probability of background IceCube events occurring

⁹⁰ The BDT score is used to reduce the atmospheric muon background, as well as separate the astrophysical signal.

⁹¹ The angular distance is motivated from IceCube multiplet searches (see Aartsen et al. 2017c).

in that time window. Given that we have at least one event detected, the p_{cluster}^{92} is the probability of that one event being in the same time window with the observed number of IceCube events, n_ν , or more from background; if there is only one IceCube event, this value is equal to 1.0. The value $p_{\text{IC},i}$ is the probability of measuring a similar or higher energy/BDT score for an IceCube event, assuming it is a background event (calculated using the energy/BDT score and zenith angle). The p_λ value is obtained by a maximum-likelihood method that measures how much the positions of the HAWC and IceCube events overlap. This is calculated as

$$\lambda(\mathbf{x}) = \sum_{i=1}^N \ln \left(\frac{S_i(\mathbf{x})}{B_i} \right), \quad (3)$$

where N is the HAWC hot spot plus the number of IceCube candidate events; S corresponds to a signal directional probability distribution function, which is assumed to be a Gaussian distribution on the sphere with a width given by the measured positional uncertainty from each detector, $S_i(\mathbf{x}) = \exp[-(\mathbf{x} - \mathbf{x}_i)^2 / 2\sigma_i^2] / (2\pi\sigma_i^2)$; and B_i is the background directional probability distribution from each detector at the position of the events. The position of the coincidence, $\mathbf{x}_{\text{coinc}}$, is defined as the position of the maximum-likelihood value, λ_{\max} , as shown in Figure 5. The uncertainty of $\mathbf{x}_{\text{coinc}}$ is calculated by the standard error $\sigma_{\mathbf{x}_{\text{coinc}}}^2 = 1/\sum_i^N (\sigma_i^{-2})$.

The λ_{\max} values are used to make a distribution of the overlap of the coincidences. A higher λ_{\max} value indicates a more significant overlap of the event uncertainties. This translates into a smaller p -value p_λ .

Due to the fact that we can have more than one IceCube event passing the selection criteria, the degrees of freedom of Equation (2) vary. We therefore calculate a p -value of the χ^2 with $6 + 2n_\nu$ degrees of freedom. The ranking statistic is then simply defined as $-\log_{10}(p\text{-value})$.

⁹² Here $p_{\text{cluster}(n_\nu)} = 1 - \sum_{i=0}^{n_\nu-2} \text{Pois}(i; f_\nu \Delta T)$, where f_ν is the IceCube background rate and ΔT is the HAWC transit time.

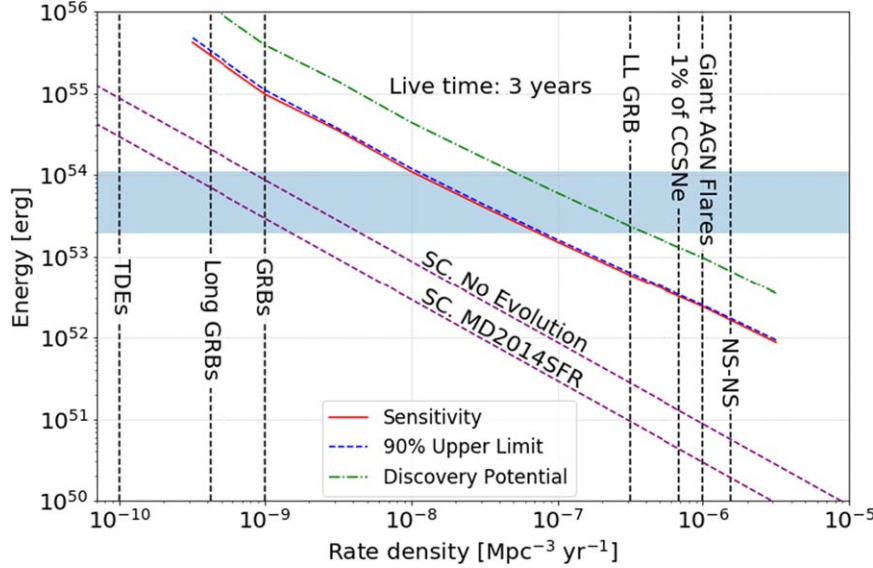


Figure 3. Sensitivity (red) and discovery potential (green) for the 3 yr of data as a function of rate density and total isotropic equivalent energy in neutrinos of transients of the order of 6 hr and assuming a power-law spectrum with an index of -2.0 . The number of coincidences below the 1 yr^{-1} FAR threshold is used as the statistic. The upper limit (blue) result is explained in Section 4.2. The results are higher by a factor of 3 if a power-law spectrum with index -2.4 is assumed (see text for more details). The light blue horizontal band corresponds to the estimated released neutrino energy of the event IceCube-170922A related to TXS 0506+056 (Aartsen et al. 2018). The purple lines are the total neutrino isotropic equivalent energy of the source as a function of rate density that would be required to produce the total observed IceCube neutrino diffuse emission with neutrino energies between 100 GeV and 10 PeV (e.g. Murase & Waxman 2016). The vertical lines correspond to different source rate densities (Farrar & Gruzinov 2009; Strolger et al. 2015; Wanderman & Piran 2015; Murase & Fukugita 2019). The comparison is valid under the assumption that the transient phenomena are of the order of hours.

3.1. Calibration of the FAR

We apply the above-described algorithm to 3 yr of scrambled data sets from both observatories. Scrambling consists of randomizing the R.A. and time values of the events many times in order to calibrate the FAR. The result of this process is shown in Figure 2. For a specific ranking statistic, we calculate the total number of coincidences above this ranking statistic value and then divide by the total amount of scrambled simulation time to get the rate. The linear fit in Figure 2 is used to estimate the FAR in real-time analyses.

3.2. Sensitivity and Discovery Potential

To put the archival results into context, we look at a simulation for transient events that can produce both neutrinos and gamma rays. We quantify the sensitivity and discovery potential for the $1 \text{ coincidence yr}^{-1}$ threshold for a live time of 3 yr of data.

We use the FIRESONG software package (Taboada et al. 2018), which simulates neutrino sources for a given local rate density of transient gamma-ray and neutrino sources, total neutrino isotropic equivalent energies, and timescales. The outcome of the simulation is a list of simulated neutrino sources with decl., redshift, and neutrino flux normalization. This is based on a power-law energy spectrum with a spectral index of -2 for the flux, in the energy range between 10 TeV and 10 PeV ,⁹³ and a time of the burst of 6 hr .⁹⁴ Using Equation (1), we can transform the normalization to a gamma-ray flux assuming photohadronic interactions. We then simulate the sources in

HAWC, also adding EBL attenuation with the model from Domínguez et al. (2011), and in addition, we draw a Poisson random number of neutrinos with an expectation value given by the source flux and IceCube’s background. Finally, we quantify the coincidence.

We calculate the sensitivity and discovery potential by running simulations for a given pair of rate density and total neutrino isotropic energy. We apply the coincidence algorithm and, after finding the signal coincidences, add them to a distribution with random coincidences. We keep the total number of coincidences the same as that of the 3 yr of data, so we remove the same number of random coincidences as injected sources. We apply this procedure several times in order to build a distribution of the number of coincidences that cross the $1 \text{ coincidence yr}^{-1}$ threshold, $N(\text{FAR} \leqslant 1)$. If no sources are injected, $N(\text{FAR} \leqslant 1)$ is a Poisson distribution with a rate of $r_B = 3.0$ (B stands for background) for the 3 yr of observations. For the sensitivity, we find the pair of parameters that will give us $r_B + r_S = 6.0$ (where S stands for signal). This corresponds to an $N(\text{FAR} \leqslant 1)$ distribution that crosses the median of the Poisson background distribution 90% of the time. For the 5σ discovery potential, we find the pair of parameters that will give a rate of $r_B + r_S = 15.7$, since this distribution will have 50% of its population with a p -value smaller than 2.87×10^{-7} with respect to the Poisson background distribution. We fit the distribution of $N(\text{FAR} \leqslant 1)$ to a Poisson function and find the best value for r_S . The pair of rate density and total neutrino isotropic energy that gives the corresponding r_S values for sensitivity or discovery potential is plotted in Figure 3. To put the sensitivity and discovery potential in context, we include diagonal lines that show the total neutrino isotropic energy as a function of the rate density that would be required to produce the total observed IceCube diffuse neutrino flux (assuming a power-law spectrum with an index of -2.5). This assumes either no evolution or star formation evolution following the Madau–Dickinson model (Madau & Dickinson 2014); it also assumes a

⁹³ The simulation was also run with a spectral index of -2.4 . Since the energy range for IceCube’s sensitivity changes with index, the range was extended from 100 GeV to 10 PeV . The sensitivity and discovery potential of the analysis are higher by a factor of 3. Figure 3 shows the result for the simulation with a spectral index of -2.0 .

⁹⁴ Since the information given by HAWC is averaged over one transit, we use this timescale for the simulations.

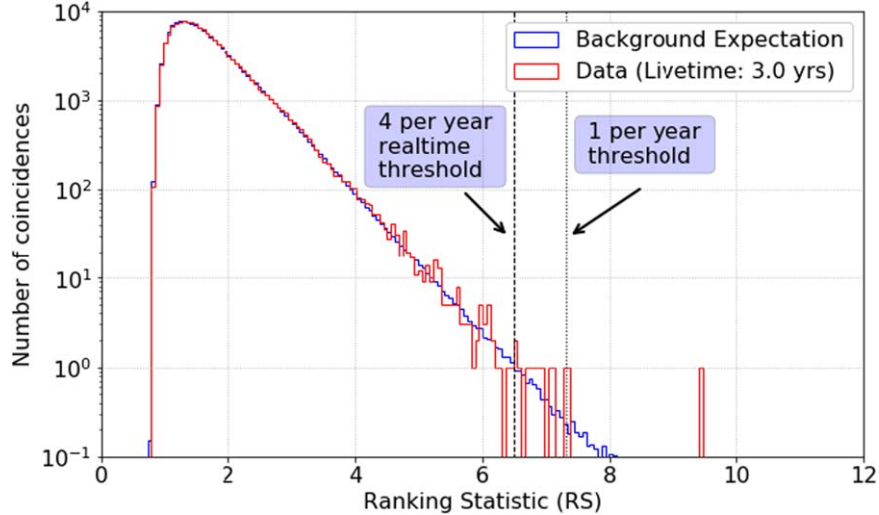


Figure 4. Ranking statistic distribution of the analysis. Blue: background expectation obtained from the scrambled data sets and normalized to the number of coincidences observed in the unblinded data set. Red: result from the unblinded analysis. Live time is 3 yr of data. The vertical lines mark 4 and 1 coincidence yr^{-1} . The highest ranking statistic in the 3 yr data set is 9.4 (one every 38.5 yr).

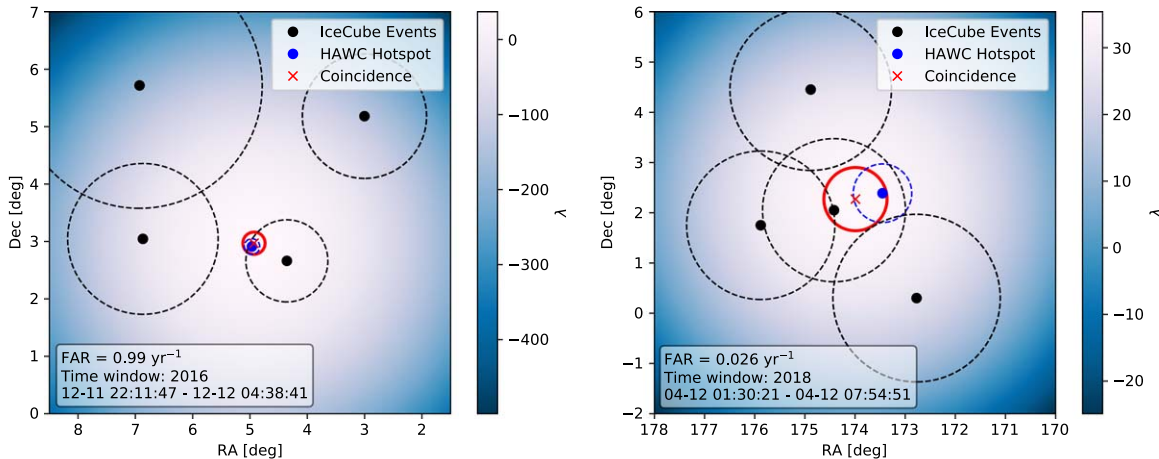


Figure 5. Sky maps of the coincidences with the lowest FAR found in the 3 yr of archival data. The positions of the individual events are marked with dots. The best-fit combined positions x_{coinc} , found after optimizing Equation (3), are marked with a cross. Circles are the 50% containment region.

Table 1
Summary Information on the Two Coincidences with $\text{FAR} < 1$

Decl. (deg)	R.A. (deg)	Uncertainty (50% Containment)(deg)	Ranking Statistic	FAR (yr^{-1})	p-value
2.96	4.93	0.16	7.3	0.99	0.95
2.27	173.99	0.53	9.4	0.026	0.075

standard candle luminosity function. Based on Aartsen et al. (2018), we marked a region in Figure 3 showing the estimated released neutrino energy of the IceCube event 170922A related to TXS 0506+056.

4. Results

4.1. Archival Data

We analyzed data collected from 2015 June to 2018 August. Figure 4 shows the distribution of the ranking statistic value of the unblinded data compared to the expected distribution of random coincidences (i.e., the scrambled data sets mentioned in Section 3).

Since we are interested in searching for rare coincidences, we look for coincidences with an FAR of less than 1 coincidence yr^{-1} , which corresponds to a ranking statistic value of 7.31. We found two coincidences, one in 2016 and one in 2018, with ranking statistics of 7.34 (1 coincidence yr^{-1}) and 9.43 (1 coincidence in 38.5 yr), respectively. These coincidences are not significant with respect to the background distribution. Using $p\text{-value} = 1 - \exp(-t \cdot \text{FAR})$, with $t = 3$ yr, the p -values are 0.95 and 0.075, respectively. The sky maps of the two coincident events with the highest ranking statistic values are shown in Figure 5. Table 1 contains the summary information on them. Information on the individual events that form each coincidence can be found in Tables 2 and 3.

Table 2
Information on the Two HAWC Hot Spots that Correspond to Each of the Coincidences with an FAR < 1 yr⁻¹ in the 3 yr Data Set

Decl. (deg)	R.A. (deg)	Uncertainty (deg)	Initial Time (UT)	Final Time (UT)	Significance σ	Flux Upper Limit (TeV ⁻¹ cm ⁻² s ⁻¹)
2.91	4.96	0.17	2016-12-11 22:11:47	2016-12-12 04:38:41	3.71	3.9e-11
2.38	173.4	0.74	2018-04-12 01:31:21	2018-04-12 07:54:51	2.77	8.3e-11

Note. Flux upper limits are based on an E^{-2} energy spectrum.

Table 3
IceCube Neutrino Information for Each of the Coincidences

Decl. (deg)	R.A. (deg)	Uncertainty (deg)	Time (UT)	Background p -value p_{IC}	$\Delta\theta$ (deg)
3.04	6.86	1.31	2016-12-11 23:20:25	0.944	1.90
2.66	4.35	0.71	2016-12-12 00:24:48	0.055	0.65
5.18	3.00	1.08	2016-12-12 01:37:28	0.391	2.99
5.71	6.92	2.13	2016-12-12 03:22:12	0.993	3.42
0.30	172.77	1.67	2018-04-12 01:57:33	0.222	2.12
4.45	174.88	1.61	2018-04-12 03:53:08	0.860	2.51
1.75	175.88	1.48	2018-04-12 04:36:11	0.001	2.50
2.05	174.42	1.42	2018-04-12 05:19:36	0.005	1.02

Note. The uncertainty corresponds to the 50% containment. Here $\Delta\theta$ is the distance from the best-fit HAWC hot-spot position to the measured neutrino position.

We looked at the SIMBAD catalog (Wenger et al. 2000) for sources that appear near the coincidences⁹⁵ and the Fermi All-sky Variability Analysis (FAVA) online tool⁹⁶ for any evidence of past flares in the region based on the light curves provided by FAVA.

For the coincidence of 2016 with an FAR of 0.99 yr⁻¹, there is a radio galaxy in the nearby region, PKS 0017+026, also known as TXS 0017+026 (Dunlop et al. 1989). This source is 0°.04 away from the best-fit position of the coincidence. Unfortunately, no distance information is available to estimate the gamma-ray attenuation. Other sources that appear nearby are quasars, but in general, these sources are too distant (redshift above 0.3), resulting in strong gamma-ray attenuation. With the FAVA tool, the source from the 3FGL catalog, J0020.9+0323, was found 0°.52 away from the best-fit coincidence position, which is outside the 50% containment region. The 3FGL catalog mentions that this is an unassociated source (Acero et al. 2015).

For the coincidence of 2018 with an FAR of 0.026 yr⁻¹, several sources appear in the SIMBAD catalog. There are nine radio galaxies within 0°.74 of the best-fit location of the coincidence from the NRAO VLA Sky Survey Catalog. From these, only NVSS J113719+022200 had some information about its distance (redshift of 0.19). We did not find nearby sources in the FAVA monitoring tool for this coincidence.

Both coincidences found with this analysis are therefore consistent with background expectations. Follow-up observations in the optical and X-ray could be helpful to discern if any of these sources are related to the coincident events.

4.2. Upper Limit

Knowing that we observed two coincidences in 3 yr of observations, we calculate an upper limit for the parameter space shown in Figure 3. We apply Poisson statistics to obtain a 90% confidence level by using Equation (9.54) in Cowan (2002). This equation gives us an upper limit on the Poisson rate of the signal based on the observation and assuming that in 3 yr of observations we expect three coincidences from background. The result is a signal Poisson rate $r_S = 3.5$, giving a total Poisson rate of $r_B + r_S = 6.5$. We use the procedure in Section 3.2 to find the corresponding upper limit values in the parameter space in Figure 3.

5. Real-time System

The real-time implementation of the analysis started on 2019 November 20. As specified in Ayala Solares et al. (2020), we use the *amony* software for the real-time implementation of the analysis. A major difference is that the system is now running on Amazon Web Services servers, which will further improve AMON’s uptime. We set a threshold for public alerts at an FAR < 4 coincidences yr⁻¹. This threshold is set so that there is a reasonable number of statistically interesting coincidences that can be followed up during a year. Alerts are sent immediately to AMON members, and a GCN notice is generated. A GCN circular is also written to inform the rest of the astrophysical community. The first public alert of the system was sent out on 2020 February 2. It had an FAR of 1.39 yr⁻¹. The reported position is (R.A., decl.) = 200°.3, 12°.71, with a 50% radius of 0°.17 (see GCN circular 26963; Ayala Solares 2020). The MASTER Global Robotic Net and the ANTARES observatory performed follow-up observations of the coincidence, but no transient event was observed (see GCN circulars 26973 and 26976; Kouchner 2020; Lipunov 2020).

⁹⁵ For the SIMBAD catalog search, we focus on sources in the 50% containment region.

⁹⁶ <https://fermi.gsfc.nasa.gov/ssc/data/access/lat/FAVA/>

The largest latency of the analysis comes from the HAWC analysis of the hot spots, since the transit needs to complete before sending that information to AMON. Based on Figure 1, the hot-spot duration can last from less than 1 hr to a bit more than 6 hr. The latency, once the data are in the AMON server, is less than 1 minute to perform the analysis and send the alert to the public.

6. Conclusion

We developed a method to search for coincidences of subthreshold data from the HAWC and IceCube observatories. Using coincidences of subthreshold data allows us to recover signal events that cannot be differentiated from the background in each individual detector. The method was tested on archival data taken between 2015 and 2018. We found two coincidences in the archival analysis that crossed the FAR threshold of 1 yr^{-1} , consistent with the background expectations of three coincidences in 3 yr. Although a few sources were found near the best coincidence positions, these results are still consistent with the expectation from random coincidences. The real-time analysis has produced one alert so far, with an FAR of 1.39 yr^{-1} . It was sent out to the community. We encourage other observatories to perform follow-up observations of these results and the real-time alerts in the future.

AMON: This research or portions of it were conducted with Advanced CyberInfrastructure computational resources provided by the Institute for Computational and Data Sciences at the Pennsylvania State University (<https://www.icds.psu.edu/>). This material is based upon work supported by the National Science Foundation under grants PHY-1708146 and PHY-1806854 and the Institute for Gravitation and the Cosmos of the Pennsylvania State University. Any opinions, findings, and conclusions or recommendations expressed in this material are those of the author(s) and do not necessarily reflect the views of the National Science Foundation. F.K. was supported as an Eberly Research Fellow by the Eberly College of Science at the Pennsylvania State University.

HAWC: We acknowledge support from the US National Science Foundation (NSF); the US Department of Energy Office of High-Energy Physics; the Laboratory Directed Research and Development (LDRD) program of Los Alamos National Laboratory; Consejo Nacional de Ciencia y Tecnología (CONACyT), México, grants 271051, 232656, 260378, 179588, 254964, 258865, 243290, 132197, A1-S-46288, A1-S-22784, cátedras 873, 1563, 341, 323, Red HAWC, México; DGAPA-UNAM grants IG101320, IN111315, IN111716-3, IN111419, IA102019, IN112218; VIEP-BUAP; PIFI 2012, 2013, PROFOCIE 2014, 2015; the University of Wisconsin Alumni Research Foundation; the Institute of Geophysics, Planetary Physics, and Signatures at Los Alamos National Laboratory; Polish Science Centre grant DEC-2017/27/B/ST9/02272; Coordinación de la Investigación Científica de la Universidad Michoacana; Royal Society—Newton Advanced Fellowship 180385; Generalitat Valenciana, grant CIDE-GENT/2018/034; and Chulalongkorn University’s CUUniverse (CUAASC) grant. Thanks to Scott Delay, Luciano Díaz, and Eduardo Murrieta for technical support.

IceCube: We gratefully acknowledge the following support: USA—US National Science Foundation Office of Polar Programs, US National Science Foundation Physics Division,

Wisconsin Alumni Research Foundation, Center for High Throughput Computing (CHTC) at the University of Wisconsin–Madison, Open Science Grid (OSG), Extreme Science and Engineering Discovery Environment (XSEDE), US Department of Energy National Energy Research Scientific Computing Center, Particle Astrophysics Research Computing Center at the University of Maryland, Institute for Cyber-Enabled Research at Michigan State University, and Astroparticle Physics Computational Facility at Marquette University; Belgium—Funds for Scientific Research (FRS-FNRS and FWO), FWO Odysseus and Big Science programs, and Belgian Federal Science Policy Office (Belspo); Germany—Bundesministerium für Bildung und Forschung (BMBF), Deutsche Forschungsgemeinschaft (DFG), Helmholtz Alliance for Astroparticle Physics (HAP), Initiative and Networking Fund of the Helmholtz Association, Deutsches Elektronen Synchrotron (DESY), and High Performance Computing Cluster of the RWTH Aachen; Sweden—Swedish Research Council, Swedish Polar Research Secretariat, Swedish National Infrastructure for Computing (SNIC), and Knut and Alice Wallenberg Foundation; Australia—Australian Research Council; Canada—Natural Sciences and Engineering Research Council of Canada, Calcul Québec, Compute Ontario, Canada Foundation for Innovation, WestGrid, and Compute Canada; Denmark—Villum Fonden, Danish National Research Foundation (DNRF), Carlsberg Foundation; New Zealand—Marsden Fund; Japan—Japan Society for Promotion of Science (JSPS) and Institute for Global Prominent Research (IGPR) of Chiba University; Korea—National Research Foundation of Korea (NRF); Switzerland—Swiss National Science Foundation (SNSF); United Kingdom—Department of Physics, University of Oxford.

Facilities: HAWC, IceCube, AMON.

Software: astropy (Price-Whelan et al. 2018), FIRESONG (Taboada et al. 2018), numpy (Van der Walt et al. 2011), scipy (Virtanen et al. 2020) matplotlib (Hunter 2007), pandas (McKinney 2010), amonpy (Ayala Solares et al. 2020).

ORCID iDs

- H. A. Ayala Solares <https://orcid.org/0000-0002-2084-5049>
- J. J. DeLaunay <https://orcid.org/0000-0001-5229-1995>
- D. B. Fox <https://orcid.org/0000-0002-3714-672X>
- T. Grégoire <https://orcid.org/0000-0001-8711-1456>
- A. Keivani <https://orcid.org/0000-0001-7197-2788>
- F. Krauß <https://orcid.org/0000-0001-6191-1244>
- M. Mostafá <https://orcid.org/0000-0002-7675-4656>
- K. Murase <https://orcid.org/0000-0002-5358-5642>
- A. Albert <https://orcid.org/0000-0003-0197-5646>
- R. Alfaro <https://orcid.org/0000-0001-8749-1647>
- K. P. Arunbabu <https://orcid.org/0000-0002-3032-663X>
- E. Belmont-Moreno <https://orcid.org/0000-0003-3207-105X>
- C. Brisbois <https://orcid.org/0000-0002-5493-6344>
- K. S. Caballero-Mora <https://orcid.org/0000-0002-4042-3855>
- A. Carramiñana <https://orcid.org/0000-0002-8553-3302>
- S. Casanova <https://orcid.org/0000-0002-6144-9122>
- U. Cotti <https://orcid.org/0000-0002-7607-9582>
- E. De la Fuente <https://orcid.org/0000-0001-9643-4134>
- B. L. Dingus <https://orcid.org/0000-0001-8451-7450>
- M. A. DuVernois <https://orcid.org/0000-0002-2987-9691>

- J. C. Díaz-Vélez  <https://orcid.org/0000-0002-0087-0693>
 C. Espinoza  <https://orcid.org/0000-0001-7074-1726>
 H. Fleischhack  <https://orcid.org/0000-0002-0794-8780>
 N. Fraija  <https://orcid.org/0000-0002-0173-6453>
 J. A. García-González  <https://orcid.org/0000-0002-4188-5584>
 F. Garfias  <https://orcid.org/0000-0003-1122-4168>
 M. M. González  <https://orcid.org/0000-0002-5209-5641>
 J. A. Goodman  <https://orcid.org/0000-0002-9790-1299>
 D. Huang  <https://orcid.org/0000-0002-3808-4639>
 F. Hueyotl-Zahuantitla  <https://orcid.org/0000-0002-5527-7141>
 A. Iriarte  <https://orcid.org/0000-0001-5811-5167>
 A. Jardin-Blicq  <https://orcid.org/0000-0002-6738-9351>
 V. Joshi  <https://orcid.org/0000-0002-1457-4027>
 H. León Vargas  <https://orcid.org/0000-0001-5516-4975>
 J. T. Linnemann  <https://orcid.org/0000-0003-2696-947X>
 A. L. Longinotti  <https://orcid.org/0000-0001-8825-3624>
 G. Luis-Raya  <https://orcid.org/0000-0003-2810-4867>
 K. Malone  <https://orcid.org/0000-0001-8088-400X>
 O. Martinez  <https://orcid.org/0000-0001-9052-856X>
 I. Martinez-Castellanos  <https://orcid.org/0000-0001-9035-1290>
 J. A. Matthews  <https://orcid.org/0000-0002-2610-863X>
 P. Miranda-Romagnoli  <https://orcid.org/0000-0002-8390-9011>
 E. Moreno  <https://orcid.org/0000-0002-1114-2640>
 L. Nellen  <https://orcid.org/0000-0003-1059-8731>
 M. Newbold  <https://orcid.org/0000-0001-9428-7572>
 M. U. Nisa  <https://orcid.org/0000-0002-6859-3944>
 R. Noriega-Papaqui  <https://orcid.org/0000-0001-7099-108X>
 E. G. Pérez-Pérez  <https://orcid.org/0000-0001-5998-4938>
 C. D. Rho  <https://orcid.org/0000-0002-6524-9769>
 D. Rosa-González  <https://orcid.org/0000-0003-1327-0838>
 F. Salesa Greus  <https://orcid.org/0000-0002-8610-8703>
 R. W. Springer  <https://orcid.org/0000-0002-1492-0380>
 K. Tollefson  <https://orcid.org/0000-0001-9725-1479>
 I. Torres  <https://orcid.org/0000-0002-1689-3945>
 L. Villaseñor  <https://orcid.org/0000-0001-6876-2800>
 A. Zepeda  <https://orcid.org/0000-0001-9976-2387>
 M. Ahlers  <https://orcid.org/0000-0003-0709-5631>
 S. BenZvi  <https://orcid.org/0000-0001-5537-4710>
 E. Bernardini  <https://orcid.org/0000-0003-3108-1141>
 P. Dave  <https://orcid.org/0000-0002-3879-5115>
 A. Desai  <https://orcid.org/0000-0001-7405-9994>
 P. Desiati  <https://orcid.org/0000-0001-9768-1858>

- P. A. Evenson  <https://orcid.org/0000-0001-7929-810X>
 A. Franckowiak  <https://orcid.org/0000-0002-5605-2219>
 S. Garrappa  <https://orcid.org/0000-0003-2403-4582>
 U. Katz  <https://orcid.org/0000-0002-7063-4418>
 A. Kheirandish  <https://orcid.org/0000-0001-7074-0539>
 H. Pandya  <https://orcid.org/0000-0002-6138-4808>
 M. Santander  <https://orcid.org/0000-0001-7297-8217>
 N. L. Strotjohann  <https://orcid.org/0000-0002-4667-6730>
 J. Vandebroucke  <https://orcid.org/0000-0002-9867-6548>
 N. Whitehorn  <https://orcid.org/0000-0002-3157-0407>

References

- Aartsen, M. G., Abraham, K., Ackermann, M., et al. 2013, *Sci*, 342, 1242856
 Aartsen, M. G., Ackermann, M., Adams, J., et al. 2017a, *JINST*, 12, P03012
 Aartsen, M. G., Ackermann, M., Adams, J., et al. 2017b, *APh*, 92, 30
 Aartsen, M. G., Ackermann, M., Adams, J., et al. 2017c, *A&A*, 607, A115
 Aartsen, M. G., Ackermann, M., Adams, J., et al. 2018, *Sci*, 361, 147
 Abbott, B. P., Abbott, R., Abbott, T. D., et al. 2017, *ApJL*, 848, L12
 Abeysekara, A. U., Albert, A., Alfaro, R., et al. 2017, *ApJ*, 843, 39
 Acero, F., Ackermann, M., Ajello, M., et al. 2015, *ApJS*, 218, 23
 Ahlers, M., & Murase, K. 2014, *PhRvD*, 90, 023010
 Ayala Solares, H. A. 2020, GCN, 26963, <https://gcn.gsfc.nasa.gov/gcn3/26963.gcn3>
 Ayala Solares, H. A., Couto, S., Cowen, D. F., et al. 2020, *APh*, 114, 68
 Ayala Solares, H. A., Cowen, D. F., DeLaunay, J. J., et al. 2019, *ApJ*, 886, 98
 Biehl, D., Boncioli, D., Fedynitch, A., et al. 2019, *EPLWC*, 208, 04002
 Cowan, G. 2002, Statistical Data Analysis (Oxford: Oxford Univ. Press)
 Domínguez, A., Primack, J. R., Rosario, D. J., et al. 2011, *MNRAS*, 410, 2556
 Dunlop, J. S., Peacock, J. A., Savage, A., et al. 1989, *MNRAS*, 238, 1171
 Farrar, G. R., & Gruzinov, A. 2009, *ApJ*, 693, 329
 Fisher, R. A. 1938, Statistical Methods for Research Workers (Edinburgh: Oliver and Boyd)
 Hunter, J. 2007, *CSE*, 9, 90
 Kouchner, A. 2020, GCN, 26976, <https://gcn.gsfc.nasa.gov/gcn3/26976.gcn3>
 Lipunov, V. 2020, GCN, 26973, <https://gcn.gsfc.nasa.gov/gcn3/26973.gcn3>
 Madau, P., & Dickinson, M. 2014, *ARA&A*, 52, 415
 McKinney, W. 2010, in Proc. 9th Python in Science Conf., ed. S. van der Walt & J. Millman, 56
 Murase, K., Ahlers, M., & Lacki, B. C. 2013, *PhRvD*, 88, 121301
 Murase, K., & Fukugita, M. 2019, *PhRvD*, 99, 063012
 Murase, K., & Waxman, E. 2016, *PhRvD*, 94, 103006
 Price-Whelan, A. M., Sipőcz, B. M., Günther, H. M., et al. 2018, *AJ*, 156, 123
 Smith, M., Fox, D., Cowen, D., et al. 2013, *APh*, 45, 56
 Strolger, L., Dahmen, T., Rodney, S. A., et al. 2015, *ApJ*, 813, 93
 Taboada, I., Tung, C. F., & Wood, J. 2018, *ICRC (Busan)*, 35, 663
 Turley, C. F. 2020a, GCN, 26674, <https://gcn.gsfc.nasa.gov/gcn3/26674.gcn3>
 Turley, C. F. 2020b, GCN, 26915, <https://gcn.gsfc.nasa.gov/gcn3/26915.gcn3>
 Turley, C. F., Fox, D. B., Keivani, A., et al. 2018, *ApJ*, 863, 64
 Van der Walt, S., Colbert, S. C., & Varoquaux, G. 2011, *CSE*, 13, 22
 Virtanen, P., Gommers, R., Oliphant, T. E., et al. 2020, *NatMe*, 17, 261
 Wanderman, D., & Piran, T. 2015, *MNRAS*, 448, 3026
 Wenger, M., Ochsenebein, F., Egret, D., et al. 2000, *A&AS*, 143, 9